Journal of Biomedical Optics

SPIEDigitalLibrary.org/jbo

Towards noncontact skin melanoma selection by multispectral imaging analysis

Ilona Kuzmina
Ilze Diebele
Dainis Jakovels
Janis Spigulis
Lauma Valeine
Janis Kapostinsh
Anna Berzina

SPIE

Towards noncontact skin melanoma selection by multispectral imaging analysis

Ilona Kuzmina,[a] Ilze Diebele,[a] Dainis Jakovels,[a] Janis Spigulis,[a] Lauma Valeine,[b] Janis Kapostinsh,[c] and Anna Berzina[d]

[a]University of Latvia, Bio-optics and Fiber Optics Laboratory, Institute of Atomic Physics and Spectroscopy, Raina Boulevard 19, Riga, LV-1586, Latvia

[b]Beauty Clinic "4th Dimension", Jeruzalemes Str. 1, Riga, LV-1010, Latvia

[c]Latvian Oncology Center, Hipokrata Str. 4, Riga, LV-1006, Latvia

[d]The Clinic of Laser Plastics, Baznicas Str. 31, Riga, LV-1010, Latvia

Abstract. A clinical trial comprising 334 pigmented and vascular lesions has been performed in three Riga clinics by means of multispectral imaging analysis. The imaging system Nuance 2.4 (CRi) and self-developed software for mapping of the main skin chromophores were used. Specific features were observed and analyzed for malignant skin melanomas: notably higher absorbance (especially as the difference of optical density relative to the healthy skin), uneven chromophore distribution over the lesion area, and the possibility to select the "melanoma areas" in the correlation graphs of chromophores. The obtained results indicate clinical potential of this technology for noncontact selection of melanoma from other pigmented and vascular skin lesions. [DOI: 10.1117/1.3584846]

Keywords: melanoma; multispectral skin chromophore mapping; pigmented and vascular skin lesions.

Paper 11093LR received Mar. 3, 2011; revised manuscript received Apr. 7, 2011; accepted for publication Apr. 11, 2011; published online Jun. 9, 2011.

Melanoma accounts for only ~4% of all skin cancers; however, it causes the greatest number of skin cancer-related deaths worldwide.[1] Optical detection/selection of skin melanomas is a hot topic in biophotonics.[2]

Multispectral imaging (MSI) is a noncontact optical technique with a promising potential for *in vivo* skin diagnostics. A set of images of the same skin location is taken, each at a different spectral band, with further analysis of spectral features at specific image areas (pixels, pixel groups). Usually multispectral images are acquired in a visible and infrared wavelength region (e.g., 400 to 970 nm) with setups based on liquid crystal tunable filters or on a series of discrete bandpass filters. Halogen lamps, incandescent lamps, or white light emitting diodes can be used as broadband illumination sources. Advanced image processing allows mapping the main skin absorbing chromophores—oxy-hemoglobin, deoxy-hemoglobin, and melanin.[3]

Address all correspondence to: Ilona Kuzmina, University of Latvia, Bio-optics and Fiber Optics Laboratory, Institute of Atomic Physics and Spectroscopy, Raina Blvd. 19, Riga, LV-1586, Latvia; Tel: 371 67228249; Fax: +371 67228249; E-mail: ilona.kuzmina@lu.lv.

The MSI technique has been previously tested for analysis of bruised skin, vascular lesions, and for automated melanoma detection.[4–7] Further, statistically significant and more detailed clinical studies are needed to identify the most reliable diagnostic criteria for specific skin lesions.

The goal of this study was to assess the potential of MSI technology for non-contact melanoma selection from other pigmented and/or vascular skin lesions. A clinical MSI trial comprising 334 lesions (including 16 melanomas) has been performed in three Riga clinics. Here we briefly present the methodology and the first results of this trial.

The experimental setup was based on multispectral imaging camera Nuance EX (CRi, USA), model–N-MSI-EX; wavelength range – 450 to 950 nm; filtering bandwidth (FWHM): 15 nm, internal liquid crystal polarizer.[8,9] Its objective was surrounded by a ring comprising three halogen lamps for skin illumination via crossed polarizer (relative to the internal one) which ensured the surface reflection cutoff.[10] The images were acquired over the whole lesion area and the near-border healthy skin in the wavelength range 450 to 950 nm with the scanning step ~10 nm and stored in a laptop. Subsequent processing of the images was performed by means of the CRi Nuance and MATLAB programs.

Before each measurement, the multispectral image of white reflectance etalon reproducing the illumination spectrum was taken. Optical density was expressed as: $\mathrm{OD}(\lambda) = -\log[I(\lambda)/I_0(\lambda)]$, where $I(\lambda)$, is the intensity of the skin-reflected light and $I_0(\lambda)$, is the intensity of the light reflected from the white etalon at the same distance (~30 cm).

Mean OD-values over the manually selected areas of the lesion and healthy skin were calculated by the CRi Nuance program. A three-chromophore absorption model was used in further image processing:

$$\mathrm{OD}(\lambda) = a_{\mathrm{HbO_2}}\varepsilon_{\mathrm{HbO_2}}(\lambda) + a_{\mathrm{Hb}}\varepsilon_{\mathrm{Hb}}(\lambda) + a_{\mathrm{mel}}\varepsilon_{\mathrm{mel}}(\lambda) + a_{\mathrm{back}}, \quad (1)$$

where $a_{\mathrm{HbO_2}}$, a_{Hb}, a_{mel} are relative concentrations of oxy-hemoglobin, deoxy-hemoglobin, and melanin with respect to the light penetration depth at the corresponding wavelength λ; $\varepsilon_{\mathrm{HbO_2}}(\lambda)$, $\varepsilon_{\mathrm{Hb}}(\lambda)$, and $\varepsilon_{\mathrm{mel}}(\lambda)$ are tabulated extinction coefficients of oxy-hemoglobin, deoxy-hemoglobin and melanin;[11,12] a_{back} is the signal of background level that was assumed equal for lesion and adjacent skin of particular patient. Relative concentrations of melanin (a_{mel}), oxy-hemoglobin ($a_{\mathrm{HbO_2}}$), and deoxy-hemoglobin (a_{Hb}) were calculated from the measurement data taken in the wavelength range 500 to 700 nm.[3]

The predicted OD spectrum (1) was fitted to the measured spectrum by solving the nonlinear least-squares problem, with subsequent determination of relative concentrations of the three skin chromophores. In addition to OD spectra, the spectra of optical density difference (δOD) between malformation and circumjacent normal skin (representing the difference of particular chromophore concentration) were calculated as:

$$\delta\,\mathrm{OD}(\lambda) = \mathrm{OD}(\lambda)_{\mathrm{malf.}} - \mathrm{OD}(\lambda)_{\mathrm{norm.skin}} = \delta a_{\mathrm{HbO_2}}\varepsilon_{\mathrm{HbO_2}}(\lambda) + \delta a_{\mathrm{Hb}}\varepsilon_{\mathrm{Hb}}(\lambda) + \delta a_{\mathrm{mel}}\varepsilon_{\mathrm{mel}}(\lambda), \quad (2)$$

1083-3668/2011/16(6)/060502/3/$25.00 © 2011 SPIE

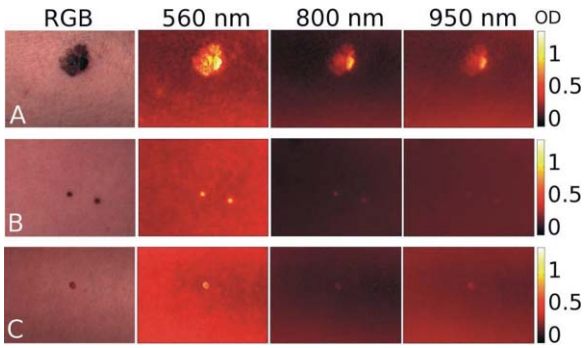

Fig. 1 RGB and spectral images of skin malformations (A: melanoma, B: nevus, and C: angioma) at three wavelength bands.

where $\delta a_{\mathrm{HbO}_2}$, δa_{Hb}, and δa_{mel} represent the relative concentration differences between the malformation and the normal skin for oxy-hemoglobin, deoxy-hemoglobin and melanin.

Overall 225 patients (186 females and 39 males) with 334 cases were inspected in three clinics under a protocol approved by the local ethics committee. The lesions were diagnosed by certified dermatologists using the Dermalite Hybrid II dermoscope. At the first phase of research described here, three groups of pathologies comprising 16 melanomas, 158 nonmalignant pigmented lesions (nevi: dysplastic—3, common—62, dermal—39, combined—12, junctional—10, papillomatic—8, congenital—6, Spilius—3, Halo—1, Meishneri—1, sebaceus—1, blue—1, ceruleus—1, acral—1, globular—1; hypermelanoses—8) and 32 nonmalignant vascular lesions (hemangiomas—30, port-wine stains—2) were selected for a more detailed study, with special attention to melanomas as the most dangerous skin malformations.

"Fading" of spectral images with increased wavelength was observed for three skin pathologies: melanomas, nevi and angiomas (Fig. 1). It may be explained by increased penetration depth in skin, resulting in decreased contrast due to larger light scattering volume. However, in the case of melanomas at 950 nm the contrast was still much higher than that for other pigmented lesions (nevi), so indicating to considerably deeper structural damage of skin. Such images reflect integral absorbance and scattering within and around the skin malformations at specific wavelengths, but they do not provide quantitative information. Clinically useful data can be obtained by analysis of the skin-remitted spectra if the pathology region is compared with the surrounding healthy skin of the same person. Multispectral scanning in the range 450 to 950 nm offers such a possibility, and a huge number of spectra from the studied pathologies were collected. To characterize the basic spectral features for each group of the malformations, the averaged spectra were calculated (Fig. 2). The spectra of vascular malformations, if compared to those of the pigmented ones, have a specific feature—the characteristic hemoglobin absorption edge in the vicinity of 600 nm. Concerning the pigmented lesions, one can note that melanomas show a notably higher relative absorption than the other pigmented malformations, and the differential OD spectra [when the OD-spectrum of the surrounding healthy skin is extracted in Fig. 2(b)] exhibit even more pronounced spectral differences. Consequently, δOD (λ) can

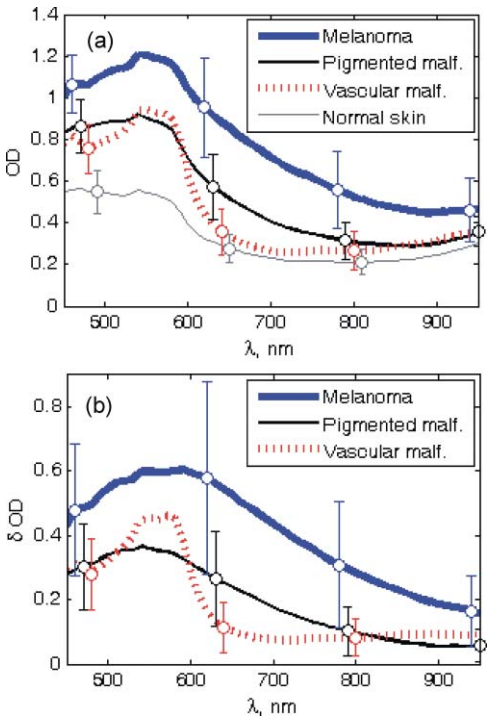

Fig. 2 The averaged OD spectra (a) and OD difference spectra (b) for melanomas, other pigmented malformations, vascular malformations, and normal skin behind the pathology border.

be regarded as a potentially sensitive parameter for melanoma detection.

Figure 3 represents the obtained chromophore maps for melanoma. The content of melanin, oxy-hemoglobin, and deoxy-hemoglobin is clearly different from that in the surrounding healthy skin. The melanin and deoxy-hemoglobin content is increased while the oxy-hemoglobin content is decreased. Melanoma exhibits uneven distribution of all three chromophores over its surface and slightly less increased deoxy-hemoglobin level.

Correlations between the calculated chromophore concentrations in malformations and normal skin were analyzed for

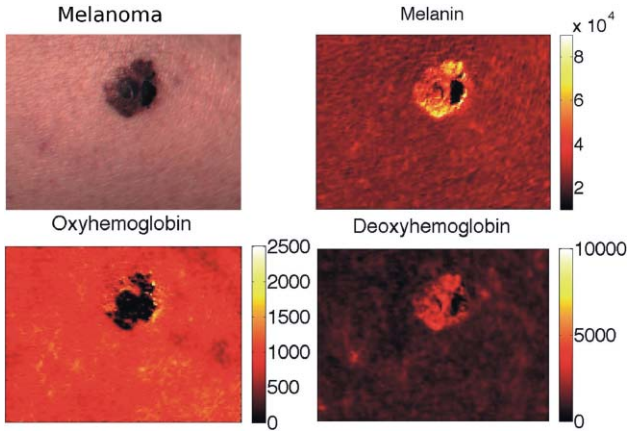

Fig. 3 The RGB image of a melanoma in comparison with the calculated relative concentration distribution maps of melanin, oxy-hemoglobin, and deoxy-hemoglobin.

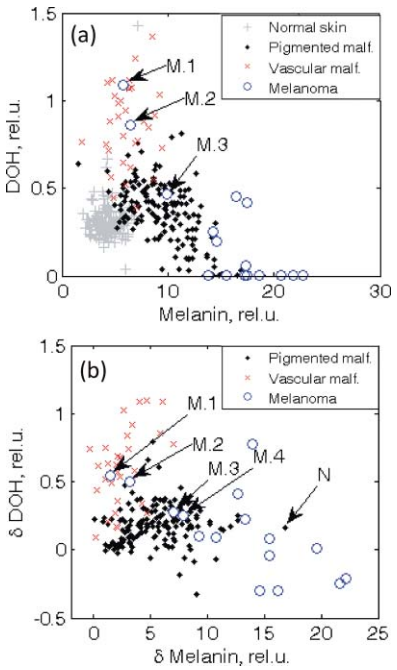

Fig. 4 The OD-correlation graph for (a) deoxy-hemoglobin: melanin with respect to the three groups of malformations (melanoma, other pigmented, and vascular) and normal skin and the δOD-correlation graph (b) for relative chromophore changes compared to normal skin. M1, M2: ulcerated melanomas on the back and the foot, M3: a melanoma on the foot, M4: a melanoma on the back, N: an intradermal nevus with hair follicles.

different chromophore pairs. In terms of OD-values, the three studied groups of pathologies (melanomas, other pigmented and vascular) seem to be best resolved in the deoxy-hemoglobin —melanin correlation graph [Fig. 4(a)]. Even better resolution of the pathology groups was achieved in a similar graph if the differential value δOD was taken as the reference parameter [Fig. 4(b)]. In fact, all points for the studied melanomas, except for four (M1–M4 in Fig. 4, M1, M2 lesions in an advanced stage—ulcerated) are well-grouped on the right side of the graphs, while the other pigmented lesions are grouped next to the left [except a nevus with hair follicles, N in Figs. 4(c) and 4(d)], with a further group of vascular malformations.

To conclude, this study revealed some interesting spectral details for three groups of skin malformations—melanomas, other pigmented lesions and benign vascular lesions. Specific features for malignant skin melanomas—appearance in near-infrared 950 nm images, a notably higher absorbance (especially as the difference of optical density relatively to the healthy skin), an uneven chromophore distribution over the lesion area, and the possibility to select "melanoma areas" in the correlation graphs of chromophores—were observed and analyzed. The previously developed three chromophore model with spectral limitation 500 to 700 nm (Ref. 3) provided qualitatively adequate skin chromophore maps for all regarded malformations; potentially, it could be helpful for assessment of skin pathologies in clinical praxis. In this model a_{back} is assumed equal for lesion and adjacent skin of a particular patient and eliminated in δOD calculations. We suppose this to be true for most patients; however, exceptions cannot be excluded, e.g., if the circumjacent skin is inflamed. During this study oxy-hemoglobin is not significantly observed. Possible reasons of this could be insufficient spectral resolution of the system, too wide selected spectral bands, and imperfect approximation due to the model does not take into account wavelength-dependent scattering and penetration depth of light.

Generally, the obtained results confirm the clinical potential of the multispectral imaging technology for noncontact quantitative assessment of melanomas and other skin a pathologies. Further improvements of the model would include more chromophores (e.g., bilirubin, water) and corrections due to wavelength-dependent scattering. It would increase the chromophore-sensitivity and, eventually, selectivity for melanoma detection. Besides, complex analysis of several features of the lesions is one of the future directions of this research.

Acknowledgments

The authors are deeply thankful for clinical support to dermatologists A. Derjabo, J. Pudova, R. Karls, L. Jacevica, and A. Abelite. This work was financially supported by European Social Fund, Project No. 2009/0211/1DP/1.1.1.2.0 /09/APIA/VIAA/077.

References

1. W. Klaus and J. R. Allen, *Fitzpatrick's Color Atlas & Synopsis of Clinical Dermatology*, McGraw-Hill Professional, New York (2009).
2. A. Garcia-Uribe, E. B. Smith, J. Zou, M. Duvic, V. Prieto, and L. V. Wang, "*In-vivo* characterization of optical properties of pigmented skin lesions including melanoma using oblique incidence diffuse reflectance spectrometry," *J. Biomed. Opt.* **16**, 020501 (2011).
3. D. Jakovels and J. Spigulis, "2-D mapping of skin chromophores in the spectral range 500–700 nm," *J. Biophot.* **3**, 125–129 (2010).
4. L. Randeberg, I. Baarstad, T. Loke, P. Kaspersen, and L. O. Svaasand, "Hyperspectral imaging of bruised skin," *Proc. SPIE* **6078**, 60780O (2006).
5. I. Kuzmina, I. Diebele, L. Asare, A. Kempele, A. Abelite, D. Jakovels, and J. Spigulis, "Multispectral imaging of pigmented and vascular cutaneous malformations: the influence of laser treatment," *Proc. SPIE* **7376**, 73760J (2010).
6. I. Kuzmina, I. Diebele, J. Spigulis, L. Valeine, A. Berzina, and A. Abelite, "Contact and contactless diffuse reflectance spectroscopy: potential for recovery monitoring of vascular lesions after intense pulsed light treatment," *J. Biomed. Opt.* **16**(4), 040505 (2011).
7. S. Tomatis, M. Carrara, A. Bono, C. Bartoli, M. Lualdi, G. Tragni, A. Colombo, and R. Marchesini, "Automated melanoma detection with a novel multispectral imaging system: results of a prospective study," *Phys. Med. Biol.* **50**, 1675–1687 (2005).
8. I. Kuzmina, I. Diebele, L. Valeine, D. Jakovels, A. Kempele, J. Kapostinsh, and J. Spigulis, "Multi-spectral imaging analysis of pigmented and vascular skin lesions: results of a clinical trial," *Proc. SPIE* **7883**, 788312 (2011).
9. *User's Manual for Nuance 2.4.*, Cambridge Research & Instrumentation, Woburn (2007).
10. S. G. Demos and R. R. Alfano, "Optical polarization imaging," *Appl. Opt.* **36**(1), 150–155 (1997).
11. S. Prahl. *Tabulated Molar Extinction Coefficient for Hemoglobin in Water*, http://omlc.ogi.edu/spectra/hemoglobin/summary.html
12. T. Sarna and H. M. Swartz, *The Physical Properties of Melanins*, http://omlc.ogi.edu/spectra/melanin/eumelanin.html